Fluid substitution in porous rocks with aligned cracks: theory versus numerical modeling

Luke Brown, Boris Gurevich and Dina Makarynska, Curtin University of Technology, Radim Ciz, CSIRO Petroleum, Christoph H. Arns and Mark A. Knackstedt, Australian National University*

Summary

The effect of penny-shaped cracks on the elastic properties of porous media is modeled using static finite element modeling (FEM) code. Anisotropic Gassmann theory is used to predict the effective properties of the saturated cracked media from their dry properties. There is an excellent agreement between numerical results and theory, with a small error associated with partially inequilibrated patches of fluid in the FEM. These patches of fluid result in a residual stiffness which can be subtracted from the FEM results to further improve agreement with Gassmann theory.

Introduction

The effect of fluid saturated cracks on the elastic properties of porous rocks differs significantly from their effect in elastic solids. In the elastic case, incompressible fluid is trapped in the isolated cracks, and effectively stiffens the cracks. In the porous case however, fluid can flow from the cracks into the pore space making the cracks more compliant. Saturated porous rocks with aligned cracks will therefore exhibit larger seismic anisotropy than their elastic counterparts.

The effective elastic properties of fluid saturated reservoirs with aligned cracks can be predicted using anisotropic Gassmann theory (Gassmann, 1951; Brown and Korringa, 1975). This theory assumes that crack size is much smaller than wavelength, but much larger than the pore structure. The effect of aligned cracks on the effective elastic properties of a porous rock may differ when the crack length and/or thickness are comparable to the pore size.

In this paper we numerically compute elastic properties of porous rocks with aligned penny-shaped cracks using static finite element modeling (FEM). The numerical results are then compared with the anisotropic Gassmann fluid substitution theory for different fluid properties.

Anisotropic Gassmann fluid substitution

The isotropic Gassmann equations, commonly used for fluid substitution in isotropic porous media, do not account for anisotropy and therefore cannot be applied in the case of aligned cracks. However, Gassmann (1951) also presented similar equations for an anisotropic medium. The well known Brown and Korringa (1975) equations are a generalization of these equations to microterogeneous and microanisotropic rocks, and are equivalent to anisotropic Gassmann equations for a rock composed of a single isotropic grain material.

Anisotropic Gassmann theory predicts the effect of a saturating fluid on the elastic properties of a porous rock with aligned cracks. These equations assume fluid pressure equilibration throughout the pore space of the rock, and are therefore only valid in the static limit (low frequency).

The relationship between elastic moduli of the dry and fluid saturated medium is given by:

$$c_{ij}^{sat} = c_{ij}^{dry} + \alpha_i \alpha_j M \,, \tag{1}$$

where

$$\alpha_i = 1 - \frac{\sum_{j=1}^{3} c_{ij}^{dry}}{3K_g}, \tag{2}$$

scalar M is the direct analog of Gassmann's pore space modulus,

$$M = \frac{Kg}{\left(1 - \frac{K^*}{K_g}\right) - \phi\left(1 - \frac{K_g}{K_f}\right)}, \tag{3}$$

K^* is the generalized bulk modulus defined as:

$$K^* = \sum_{i=1}^{3}\sum_{j=1}^{3} c_{ij}^{dry} \,, \tag{4}$$

K_g and K_f are the bulk moduli of the grain and fluid constituents respectively, ϕ is porosity, and c^{dry} are the components of the stiffness matrix of the dry medium. An isotropic porous background with a single set of rotationally invariant fractures is a transversely isotropic (TI) medium with five independent elastic constants.

Assuming the rock is transversely isotropic with symmetry axis in the x_3 direction, equation (2) gives:

$$\alpha_3 = 1 - \frac{c_{33}^{dry} + 2c_{13}^{dry}}{3K_g} \,,$$

$$\alpha_1 = \alpha_2 = 1 - \frac{c_{11}^{dry} + c_{12}^{dry} + c_{13}^{dry}}{3K_g} \,, \tag{5}$$

$$\alpha_4 = \alpha_5 = \alpha_6 = 0 \,.$$

Given the properties of the dry rock, grain and fluid, this set of equations will predict the effective elastic properties of the same rock saturated with any given Newtonian fluid.

The dry stiffness matrix for a rock with aligned cracks can be obtained by using the linear slip model (Schoenberg and Douma, 1998). By combining anisotropic Gassmann theory with the linear slip model, Gurevich (2003) derived explicit expressions for the saturated stiffness components in terms of background, grain and fluid properties, as well as normal and tangential fracture weakness. However, this approach is only applicable for "true" fractures whose lateral dimensions are much larger than their thickness, e.g., for penny-shaped cracks with aspect ration <0.001. Here we consider cracks with aspect ratio on the order of 0.1, where this approach would be inaccurate.

In this study determine the dry stiffness components directly from the numerical results for the dry case. The properties of the background (K_g and ϕ) and fluid (K_f) are also known (input parameters for FEM). The anisotropic Gassmann equations can therefore be used to predict the elastic properties of the saturated medium.

Finite element modeling

The FEM algorithm was originally written by Garboczi and Day (1995) and adopted for the study of porous rocks by Arns et al. (2002). The algorithm uses a formulation of the static linear elastic equations, and finds the steady state solution by minimising the strain energy of the system.

For an isotropic model, one run with a single set of input strains is sufficient to determine the two independent elastic coefficients. By running the same model several times with different initial strain conditions, we can use this algorithm to determine the elastic properties of anisotropic models. For our case of transverse isotropy, we only need to run the model twice in order to calculate the five elastic constants.

Input is typically a 2D or 3D array, with each element representing a pixel from a high resolution CT scan (digital core) or a synthetically generated model. The background model used in this study was synthetically generated using a random distribution of overlapping spheres (Figure 1). Collision detection was used to ensure connectivity within the solid phase, i.e. no floating grains which would prevent convergence to a steady state.

A sufficient number of spherical grains is needed to make the background statistically isotropic, however using too many grains reduces porosity and has a detrimental effect on fluid communication within the model. The background model used in this study was chosen for its relatively high porosity (~25%) and good P-wave isotropy. Quartz was used as the grain material (Kg=37GPa and μ=44GPa).

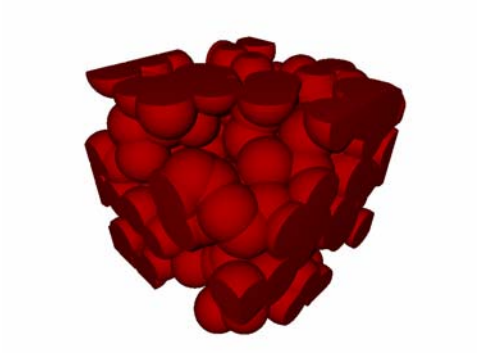

Figure 1: Isotropic background of random overlapping spheres.

A single set of aligned, randomly distributed, penny-shaped cracks is inserted within the porous background. Penny-shaped cracks are thin spheroids with semi-axes satisfying the geometry $a_2 = a_3 >> a_1$. The two important quantities used to describe penny-shaped cracks are aspect ratio, $\alpha=a_1/a_2$, and crack density,

$$e = \frac{Na_2^3}{V} = \frac{3\phi_c}{4\pi\alpha},$$

where n is number of cracks in volume V, and ϕ_c is crack porosity. The cracks used in the FEM are 3 elements thick and 25 elements in diameter giving an aspect ratio of 0.12.

Results

The numerical simulations were run for fluid bulk modulus K_f ranging from 0-3GPa, and crack density e ranging from 0-0.9. The elastic properties for each case were calculated using Hooke's law to relate the average stress and strain, $\sigma = \mathbf{c}\varepsilon$, where $\mathbf{c}$ is the complete stiffness matrix.

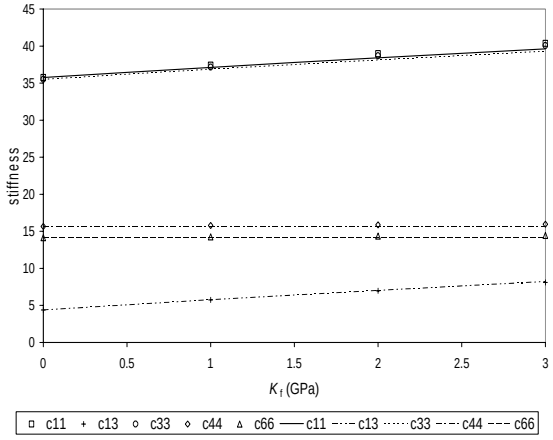

Figure 2: Stiffness components for porous background model as a function of fluid modulus. Symbols are FEM results and lines are anisotropic Gassmann predictions.

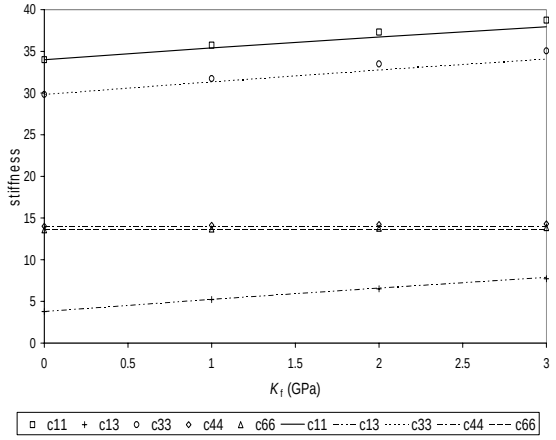

Figure 3: Stiffness components for cracked porous model as a function of fluid modulus. Symbols are FEM results and lines are anisotropic Gassmann predictions.

The stiffness components are shown as a function of fluid bulk modulus in Figure 2 for the non-cracked background, and in Figure 3 for a constant crack density of ~0.05.

Discussion

The results for the non-cracked background model (Figure 2) show that the background is practically isotropic; there is only a small difference between stiffness components c_{44} and c_{66}, equivalent to shear modulus μ. These components do not change with fluid saturation which is consistent with the isotropic Gassmann theory.

There is good agreement between the numerical results and the saturated properties predicted using isotropic Gassmann fluid substitution. Since the theory is fitted to the dry FEM results there is obviously a perfect fit at that point (K_f=0). However, there is a small error in the fit which increases with increasing fluid bulk modulus.

The results for the cracked model (Figure 3) show that the aligned cracks cause significant anisotropy. This is clearly seen as the model is much more compliant parallel to the axis of symmetry (c_{33} direction), and the normal stiffness components c_{11} and c_{33} diverge.

Also shown in Figure 3 are the predictions of anisotropic Gassmann theory, equations (1)-(5). Again there is a good agreement between the numerical results and theory. The error is approximately the same magnitude for both the non-cracked and cracked models, indicating that it is not related to the presence of the cracks. Given the error seems to be directly proportional to K_f, it is thought to be the result of partially inequilibrated fluid pressure.

This effect can be investigated using the simple model shown in Figure 4, essentially four outer chambers filled with fluid connected via channels of square cross-section to a single central chamber filled with a different fluid. The total cross-section area of the channels is kept constant, but changing the size of individual channels affects the fluid relaxation within the model. The model with large channels (right) achieves a relaxed state with pressure equilibrated between the two fluid phases. For the model with many small channels (left) however, the algorithm is unable to equilibrate pressure between the two fluids.

The same mechanism would allow small pore channels in the porous model to effectively isolate patches of fluid and prevent them from relaxing with the rest of the fluid phase. These partially relaxed fluid zones would leave residual fluid stiffness, which would increase proportionally with fluid modulus as observed in our results.

This fluid communication problem could be minimized by using larger models with increased resolution of pore channels, but this becomes prohibitive due to cubic increase in required memory and computation time.

By assuming that the cracks are well connected to the porous background and do not effect the error, a correction can be derived from the background error and applied to the cracked case. The numerical results for the isotropic background should equal the isotropic Gassmann theory if the residual fluid stiffness is removed, so that:

$$c_{ij}^{FEM} - c_{ij}^{RFS} = c_{ij}^{GASS} .$$

The above expression is a function of K_f. Subtracting the Gassmann results $\mathbf{c}^{GASS}$ from the numerical results $\mathbf{c}^{FEM}$, gives the residual fluid stiffness $\mathbf{c}^{RFS}$. The residual fluid stiffness can then subtracted from the numerical results for the cracked case to approximate the fully relaxed state.

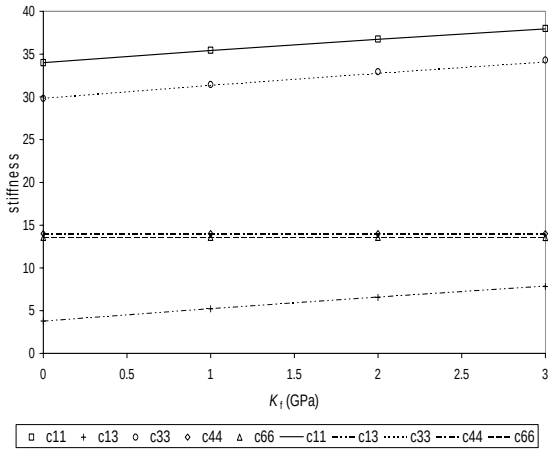

Figure 5: Stiffness components for cracked porous model after correction for partial fluid relaxation. Symbols are corrected FEM results and lines are anisotropic Gassmann predictions.

The results for the cracked model following this correction are shown in Figure 5. The fit between the numerical results and anisotropic Gassmann theory is much better for higher values of fluid modulus.

Although the correction works well in this case, the fluid in smaller cracks may not equilibrate with the background, or larger cracks could potentially form open channels to fluid patches which were isolated in the background model. In these cases this correction would not be applicable.

Conclusions

The saturated elastic properties of porous rock with aligned cracks predicted by anisotropic Gassmann theory agree with our FEM results. There is a small error in the FEM results caused by imperfect fluid pressure equilibration throughout the pore and crack space. We are currently developing a numerical technique to address this issue.

References

Arns, C., Knackstedt, M., Pinczewskiz, W., Garboczi, E., 2002, Computation of linear elastic properties from microtomographic images: Methodology and agreement between theory and experiment: Geophysics, 67, 5, 1396-1405.

Brown, R.J.S., and Korringa, J., 1975, On the dependence of the elastic properties of a porous rock on the compressibility of the pore fluid: Geophysics, 40, 608-616.

Garboczi, E. J., and Day, A. R., 1995, An algorithm for calculating the effective linear elastic properties of heterogeneous materials: Three dimensional results for composites with equal phase poisson ratios: J. Mech. Phys. Solids, 43, 1349–1362.

Gassmann, F., 1951, Über die Elastizität poröser Medien: Viertel. Naturforsch. Ges. Zürich, 96, 1-23.

Gurevich, B., 2003, Elastic properties of saturated porous rocks with aligned fractures: J. Appl. Geoph., 54, 203-218.

Acknowledgments

The work of Luke Brown was supported by WACUPS Postgraduate Scholarship. The work of Radim Ciz was supported by CSIRO Postdoctoral Fellowship. The study was partially funded by Australian Research Council Discovery-Project DP0342998.

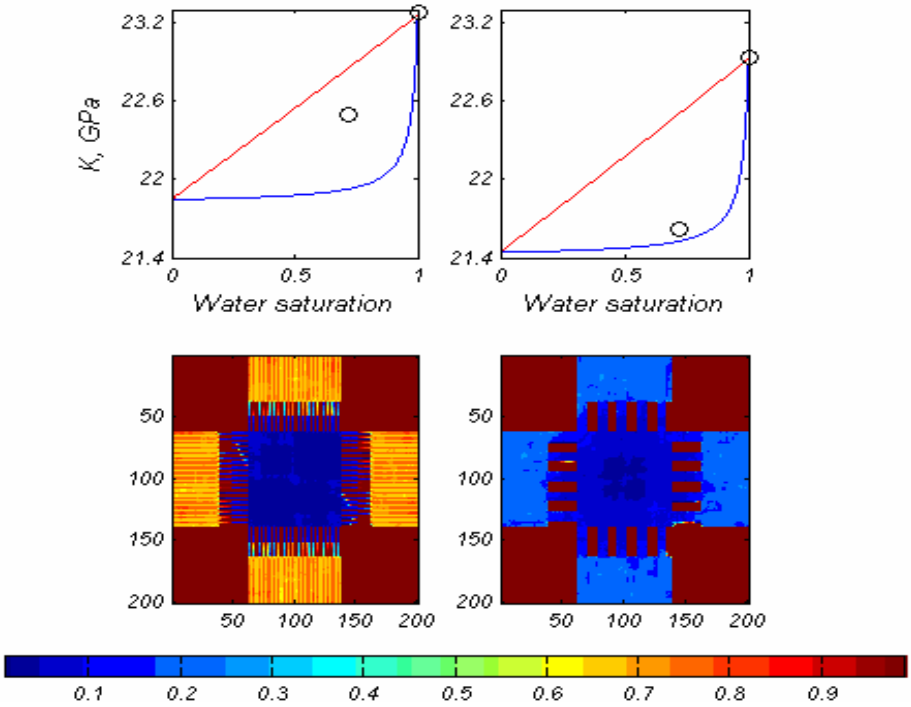

Figure 4: Simple model for simulation of fluid relaxation in porous structures (brown is solid phase). Top panels show numerical result relative to the Biot-Gassmann-Hill (red line) and Biot-Gassmann-Wood (blue line) limits. Colors in bottom panels represent normalized fluid pressure at end of the relaxation process (middle slice through the model).

EDITED REFERENCES

Note: This reference list is a copy-edited version of the reference list submitted by the author. Reference lists for the 2006 SEG Technical Program Expanded Abstracts have been copy edited so that references provided with the online metadata for each paper will achieve a high degree of linking to cited sources that appear on the Web.

REFERENCES

Arns, C., M. Knackstedt, W. Pinczewskiz, and E. Garboczi, 2002, Computation of linear elastic properties from microtomographic images: Methodology and agreement between theory and experiment: Geophysics, **67**, 1396–1405.

Brown, R. J. S., and J. Korringa, 1975, On the dependence of the elastic properties of a porous rock on the compressibility of the pore fluid: Geophysics, **40**, 608–616.

Garboczi, E. J., and A. R. Day, 1995, An algorithm for calculating the effective linear elastic properties of heterogeneous materials: Three dimensional results for composites with equal phase Poisson ratios: Journal of the Mechanics and Physics of Solids, **43**, 1349–1362.

Gassmann, F., 1951, Über die Elastizität poröser Medien: Viertel. Naturforsch. Ges. Zürich, **96**, 1–23.

Gurevich, B., 2003, Elastic properties of saturated porous rocks with aligned fractures: Journal of Applied Geophysics, **54**, 203–218.